Analysis of the dam-foundation joint through the cohesive frictional crack model

F. Barpi & S. Valente
Dipartimento di Ingegneria Strutturale e Geotecnica, Politecnico di Torino, Torino.

ABSTRACT: The mechanical behaviour of joints plays a key role in concrete dam engineering since the joint is the weakest point in the structure and therefore the evolutionary crack process occurring along this line determines the global load bearing capacity. The reference volume involved in the above mentioned process is so large that it cannot be tested in a laboratory: a numerical model is needed. The use of the asymptotic expansions proposed by Karihaloo and Xiao 2008 at the tip of a crack with normal cohesion and Coulomb friction can overcome the numerical difficulties that appear in large scale problems when the Newton-Raphson procedure is applied to a set of equilibrium equations based on ordinary shape functions (Standard Finite Element Method). In this way it is possible to analyse problems with friction and crack propagation under the constant load induced by hydromechanical coupling. For each position of the fictitious crack tip, the condition $K_1 = K_2 = 0$ allows us to obtain the external load level and the tangential stress at the tip. If the joint strength is larger than the value obtained, the solution is acceptable, because the tensile strength is assumed negligible and the condition $K_1 = 0$ is sufficient to cause the crack growth. Otherwise the load level obtained can be considered as an overestimation of the critical value and a special form of contact problem has to be solved along the fictitious process zone. For the boundary condition analysed (ICOLD benchmark on gravity dam model), after an initial increasing phase, the water lag remains almost constant and the maximum value of load carrying capacity is achieved when the water lag reaches its constant value.

1 INTRODUCTION

The mechanical behaviour of joints plays a key role in concrete dam engineering since the joint is the weakest point in the structure and therefore the evolutionary crack process occurring along this line determines the global load bearing capacity. In the scientific literature two problems are discussed:

- the problem of sliding along a pre-existing compressed discontinuity (see, among others, Gens, Carol, and Alonso 1990),

- the problem of crack initiation and propagation along an undamaged interface (see Carol, Prat, and Lopez 1997, Červenka, Kishen, and Saouma 1998, Barpi and Valente 2008).

The latter problem is discussed below in the framework of the cohesive crack models, introduced by Barenblatt and Dugdale for elastoplastic materials, and by Hillerborg et al. for quasi-brittle materials. In this model, the nonlinear fracture process zone (due to degradation mechanisms such as plastic micro-voiding or micro-cracking) in front of the actual crack tip is lumped into a discrete line (two-dimensional) or plane (three-dimensional) and is represented by a traction-separation law across this line or plane. When the tangential components of the tractions are present the solution can lose uniqueness. Therefore numerical difficulties occur if the Newton-Raphson procedure is applied to a set of equilibrium equations based on ordinary shape functions (Standard Finite Element Method). In order to overcome these difficulties Strouboulis, Copps, and Babuska 2001 suggest constructing an approximation which employs knowledge about the character of the solution (Generalized Finite Element Method). In this direction we take advantage from the work of Karihaloo and Xiao 2008 on the asymptotic fields at the tip of a cohesive crack. In this model frictional forces operate when the crack faces are open. Therefore these forces are different from those operating in a contact problem. In this context Karihaloo and Xiao 2008 obtained asymptotic expansions at a cohesive crack tip analogous to the Williams (1957) expansions at a traction-free crack tip for any traction-separation law that can be expressed in a special polynomial form.

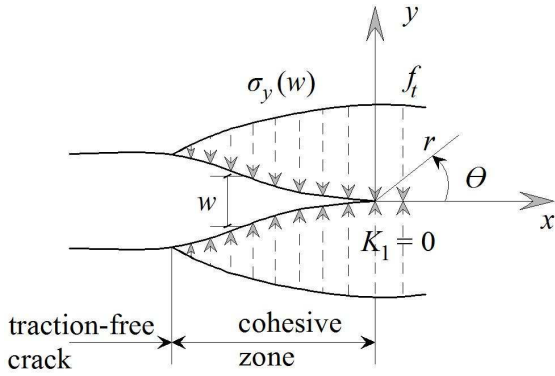## 2 POLYNOMIAL COHESIVE LAW FOR QUASI-BRITTLE MATERIALS

Figure 1. Stresses near the crack tip.

Figure 2. Non dimensional opening (w/w_c) vs. non dimensional stress (σ/σ_c).

In order to obtain the separable asymptotic field at a cohesive crack tip (in terms of r and θ functions, see Fig. 1) in quasi-brittle materials, Karihaloo and Xiao 2007 reformulate the softening law into the following polynomial form:

$$\frac{\sigma_y}{f_t} = 1 + \sum_{i=1}^{5} \alpha_i \left(\frac{w}{w_c}\right)^{\frac{2i}{3}} - \left(1 + \sum_{i=1}^{5} \alpha_i\right)\left(\frac{w}{w_c}\right)^{4} \quad (1)$$

where σ_y and f_t are the stress normal to the cohesive crack face and the uniaxial tensile strength, respectively; w and w_c are the opening displacement of the cohesive crack faces and the critical displacement at the real crack tip; α_i are fitting parameters. Equation 1 can represent a wide variety of softening laws. For example, Karihaloo and Xiao 2007 showed that the experimental results of Cornelissen, Hordijk, and Reinhardt 1986 for normal concrete can be fitted very well by Eq. 1 with:$\alpha_1 = -0.872$, $\alpha_2 = -16.729$, $\alpha_3 = 67.818$, $\alpha_4 = -110.462$, $\alpha_5 = 83.158$ (see Fig. 2). The above mentioned shape coefficients are used in the present work.

3 ASYMPTOTIC FIELDS AT THE TIP OF A CRACK WITH NORMAL COHESION AND COULOMB FRICTION

The mathematical formulation follows closely that used by Karihaloo and Xiao 2008, so only a brief description will be given here. Muskhelishvili (1953) showed that, for plane problems, stresses and displacements in the Cartesian coordinate system (see e.g. Fig. 1) can be expressed in terms of two analytic functions $\phi(z)$ and $\chi(z)$ of the complex variable $z = re^{i\theta}$

$$\sigma_x + \sigma_y = 2[\phi'(z) + \overline{\phi'(z)}] \quad (2)$$

$$\sigma_y - \sigma_x + 2i\tau_{xy} = 2[\bar{z}\phi''(z) + \chi''(z)] \quad (3)$$

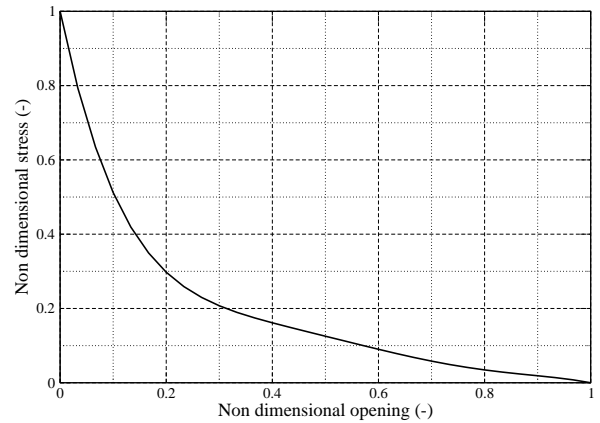$$2\mu(u + iv) = k\phi(z) - z\overline{\phi'(z)} - \overline{\chi'(z)} \quad (4)$$

where a prime denotes differentiation with respect to z and an overbar complex conjugate. In Eq. 4, $\mu = E/[2(1 + \nu)]$ is the shear modulus; the Kolosov constant is $\kappa = 3 - 4\nu$ for plane strain and $\kappa = (3 - \nu)/(1 + \nu)$ for plane stress; E and ν are Young's modulus and Poisson's ratio, respectively.

For a general mixed mode I+II problem, the two analytic functions $\phi(z)$ and $\chi(z)$ can be chosen as series of complex eigenvalue Goursat functions (Sih and Liebowitz 1968)

$$\phi(z) = \sum_{n=0}^{} A_n z^{\lambda_n} = \sum_{n=0}^{} A_n r^{\lambda_n} e^{i\lambda_n\theta}$$

$$\chi(z) = \sum_{n=0}^{} B_n z^{\lambda_n+1} = \sum_{n=0}^{} A_n r^{\lambda_n+1} e^{i(\lambda_n+1)\theta} \quad (5)$$

where the complex coefficients are $A_n = a_{1n} + ia_{2n}$ and $B_n = b_{1n} + ib_{2n}$. The eigenvalues λ_n and coefficients a_{1n}, a_{2n}, b_{1n} and b_{2n} are real.

Substituting complex functions 5 into 2, 3 and 4, the complete series expansions of the displacements and stresses near the tip of the crack can be written:

$$2\mu u = \sum_{n=0}^{} r^{\lambda_n}\Big\{k(a_{1n}\cos\lambda_n\theta -$$

$$a_{2n}\sin\lambda_n\theta) + \lambda_n[-a_{1n}\cos(\lambda_n - 2)\theta +$$

$$a_{2n}\sin(\lambda_n - 2)\theta + (\lambda_n + 1)(-b_{1n}\cos\lambda_n\theta +$$

$$b_{2n}\sin\lambda_n\theta)\Big\} \quad (6)$$

277

$$2\mu v = \sum_{n=0} r^{\lambda_n} \Big\{ k(a_{1n} \sin \lambda_n \theta -$$

$$a_{2n} \cos \lambda_n \theta) + \lambda_n [a_{1n} \sin(\lambda_n - 1)\theta +$$

$$a_{2n} \cos(\lambda_n - 2)\theta + (\lambda_n + 1)(b_{1n} \sin \lambda_n \theta +$$

$$b_{2n} \cos \lambda_n \theta) \Big\} \quad (7)$$

$$\sigma_x = \sum_{n=0} r^{\lambda_n - 1} \Big\{ 2\lambda_n [a_{1n} \cos(\lambda_n - 1)\theta$$

$$- a_{2n} \sin(\lambda_n - 1)\theta] - \lambda_n(\lambda_n - 1)[a_{1n} \cos(\lambda_n - 3)\theta$$

$$- a_{2n} \sin(\lambda_n - 3)\theta] - (\lambda_n + 1)\lambda_n [b_{1n} \cos(\lambda_n - 1)\theta$$

$$- b_{2n} \sin(\lambda_n - 1)\theta] \Big\} \quad (8)$$

$$\sigma_y = \sum_{n=0} r^{\lambda_n - 1} \Big\{ 2\lambda_n [a_{1n} \cos(\lambda_n - 1)\theta$$

$$- a_{2n} \sin(\lambda_n - 1)\theta] + \lambda_n(\lambda_n - 1)[a_{1n} \cos(\lambda_n - 3)\theta$$

$$- a_{2n} \sin(\lambda_n - 3)\theta] + (\lambda_n + 1)\lambda_n [b_{1n} \cos(\lambda_n - 1)\theta$$

$$- b_{2n} \sin(\lambda_n - 1)\theta] \Big\} \quad (9)$$

$$\tau_{xy} = \sum_{n=0} r^{\lambda_n - 1} \Big\{ \lambda_n(\lambda_n - 1)[a_{1n} \sin(\lambda_n - 3)\theta$$

$$- a_{2n} \cos(\lambda_{n-3})\theta] + (\lambda_n + 1)\lambda_n [b_{1n} \sin(\lambda_n - 1)\theta$$

$$- b_{2n} \cos(\lambda_n - 1)\theta] \Big\} \quad (10)$$

$$w = v\Big|_{\theta=\pi} - v\Big|_{\theta=-\pi} =$$

$$\sum_{n=0} \frac{r^{\lambda_n}}{\mu} [(k + \lambda_n)a_{1n} + (\lambda_n + 1)b_{1n}] \sin \lambda_n \pi \quad (11)$$

$$\delta = u\Big|_{\theta=\pi} - u\Big|_{\theta=-\pi} =$$

$$\sum_{n=0} \frac{r^{\lambda_n}}{\mu} [(\lambda_n - k)a_{2n} + (\lambda_n + 1)b_{2n}] \sin \lambda_n \pi \quad (12)$$

The imposition of continuity conditions on normal stress component of Eq. 9 ($\sigma_y|_{\theta=\pi} = \sigma_y|_{\theta=-\pi}$) along the cohesive zone gives:

$$(a_{2n} + b_{2n}) \sin(\lambda_{n-1})\pi = 0 \quad (13)$$

The imposition of continuity conditions on tangential stress component of Eq. 10 ($\tau_{xy}|_{\theta=\pi} = \tau_{xy}|_{\theta=-\pi}$) along the cohesive zone gives:

$$[(\lambda_n - 1)a_{1n} + (\lambda_{n+1})b_{1n}] \sin(\lambda_n - 1)\pi = 0 \quad (14)$$

Equations 13 and 14 are satisfied for $\sin(\lambda_n - 1)\pi = 0$ or for $b_{2n} = -a_{2n}$. In other words the asymptotic solutions can be collected in two classes. The first class is characterized by integer eigenvalues:

$$\lambda_n = n + 1, \quad n = 0, 1, 2\ldots, \quad w = 0, \quad \delta = 0 \quad (15)$$

the second class is characterized by the remaining cases (non integer eigenvalues):

$$b_{2n} = -a_{2n}, \quad b_{1n} = -\frac{\lambda_n - 1}{\lambda_n + 1}a_{1n}, \quad w \neq 0, \quad \delta \neq 0 \quad (16)$$

The imposition of the Coulombian friction condition ($\tau_{xy}|_{\theta=\pi} = -\mu_f \sigma_y|_{\theta=\pi}$) along the cohesive zone, for the first class of solutions gives:

$$\lambda_n = n + 1$$

$$na_{2n} + (n + 2)b_{2n} = -\mu_f(n + 2)(a_{1n} + b_{1n})$$

$$n = 0, 1, 2\ldots \quad (17)$$

and for the second class of solutions gives:

$$(\mu_f a_{1n} - a_{2n}) \cos(\lambda_n - 1)\pi = 0 \quad (18)$$

Since both factors in Eq. 18 may vanish independently of each other, it appears that, for the crack with normal cohesion and Coulombian friction, the eigenvalues and asymptotic fields are not unique. Additional assumptions have to be made to ensure uniqueness. Assuming that $\mu_f a_{1n} - a_{2n} \neq 0$, Eq. 18 gives:

$$\cos(\lambda_n - 1)\pi = 0, \quad \lambda_n = \frac{2n + 3}{2}, \quad n = 0, 1, 2\ldots \quad (19)$$

This assumption does not lead to any loss of generality. Now it is possible to complete the expressions of the asymptotic fields.

In the case of integer eigenvalues, substituting Eq. 17 in 9 gives:

$$\sigma_y|_{\theta=\pm\pi} = -\frac{\tau_{xy}|_{\theta=\pm\pi}}{\mu_f} =$$

$$\sum_{n=1} (n + 2)(n + 1)r^n (a_{1n} b_{1n}) \cos(n\pi) \quad (20)$$

In the case of non-integer eigenvalues, substituting Eqs. 16 and 19 in 11 and 12 gives:

$$w = \sum_{n=0} \frac{r^{\frac{2n+3}{2}}}{\mu} \left[\left(\kappa + \frac{2n+3}{2} \right) a_{1n} + \frac{2n+5}{2} b_{1n} \right]$$

$$\sin \frac{2n+3}{2} \pi \quad (21)$$

$$\delta = \sum_{n=0} \frac{r^{\frac{2n+3}{2}}}{\mu} \left[\left(\frac{2n+3}{2} - \kappa \right) a_{2n} + \frac{2n+5}{2} b_{2n} \right]$$

$$\sin \frac{2n+3}{2} \pi \quad (22)$$

In Eq. 19 $n = -1$ corresponds to the singular terms, which are excluded a priori ($K_1 = K_2 = 0$).

4 THE ITERATIVE SOLUTION PROCEDURE

For each position of the fictitious crack tip (shortening FCT) the following iterative procedure is applied:

$$\begin{bmatrix} w \\ \delta \end{bmatrix}^{i+1} = f\left(\begin{bmatrix} \sigma_y \\ \tau_{xy} \end{bmatrix}^i \right)$$

$$\begin{bmatrix} \sigma_y \\ \tau_{xy} \end{bmatrix}^{i+1} = g\left(\begin{bmatrix} w \\ \delta \end{bmatrix}^{i+1} \right) \quad i = 0, 1, 2 \dots \quad (23)$$

Since the material outside the fracture process zone (shortening FPZ) is linear, it is possible to compute the external load multiplier (λ) and the tangential stress at the FCT ($\tau_{xy,FCT}$) by imposing that the stress field is not singular (stress intensity factors $K_1 = K_2 = 0$). All these linear constraints are included in the operator f.

Since $w, \delta, \sigma_y, \tau_{xy}$ are compatible with the asymptotic solution, operator g includes the constraints described in Karihaloo and Xiao 2008 and not repeated here.

At the first iteration ($i = 0$) $w = \delta = 0$ is assumed along the FPZ. According to this approach λ and $\tau_{xy,FCT}$ are not defined *a priori* but are obtained from the analysis related to a pre-defined position of the FCT. If $\tau_{xy,FCT}$ is less than or equal to the local critical value, the solution obtained can be accepted. On the contary, if $\tau_{xy,FCT}$ exceeds the local critical value, the associated load level can be seen as an overestimation of the real critical value which remains unknown. Of course it is possible to reduce the load level but in that case K_1 becomes negative, a contact problem arises along the FPZ and the dilatancy condition has to be imposed. This special form of contact problem is beyond the scope of the present work.

In the well established literature on mechanical behaviour of concrete joints (see Červenka, Kishen, and Saouma 1998), softening depends only on $w_{eff} = \sqrt{w^2 + \delta^2}$. In the asymptotic expansion used, softening depends only on w. Therefore, during the iterative procedure, w_c changes as follows:

$$w_c^{i+1} = \sqrt{w_{eff,c}^2 - (\delta^i)^2} \quad (24)$$
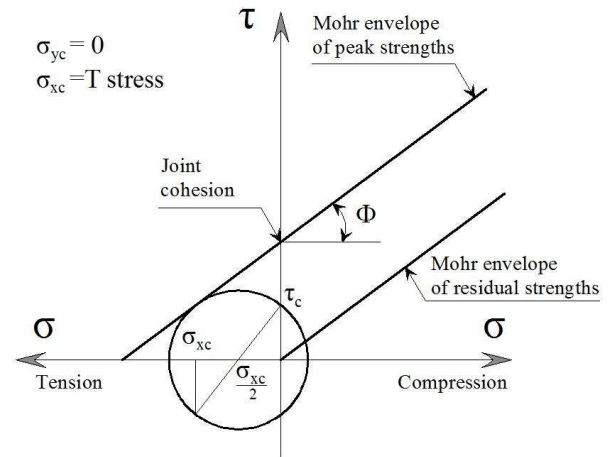
5 NUMERICAL EXAMPLE

Figure 3. Failure criterion.

As an example of application, the benchmark problem proposed in 1999 by the International Commission On Large Dams ICOLD 1999 was analysed (dam height 80m, base 60m, see Fig. 4).

For simplicity the same value of Young's modulus ($E = 32.5$ GPa) and Poisson's ratio ($\nu = 0.125$) was assumed. Figure 3 shows the Mohr envelope of peak and residual strength for the joint (cohesion=0.7MPa, $\Phi = 30^o$). The stress σ_x is positive (tension) along the lower edge of the crack. Figure 3 shows its contribution to the achievement of the critical condition. As the crack grows, the value of σ_x at the FCT (also called T-stress) reduces. For conservative reasons, the tensile strength of the joint and the related fracture energy are assumed as negligible. In case of linear softening the ICOLD benchmark suggests the assumption of a critical value of the crack sliding displacement equal to $\delta_c = 1$ mm. Since the shape of the softening law assumed in the present paper is based on the results of Cornelissen, Hordijk, and Reinhardt 1986, the previous value was increased to δ_c=2.56 mm. This choice is motivated by keeping constant the fracture energy G_F^{II} in the case $w = 0$. Since the crack is open, beyond this value no stress transfer occurs.
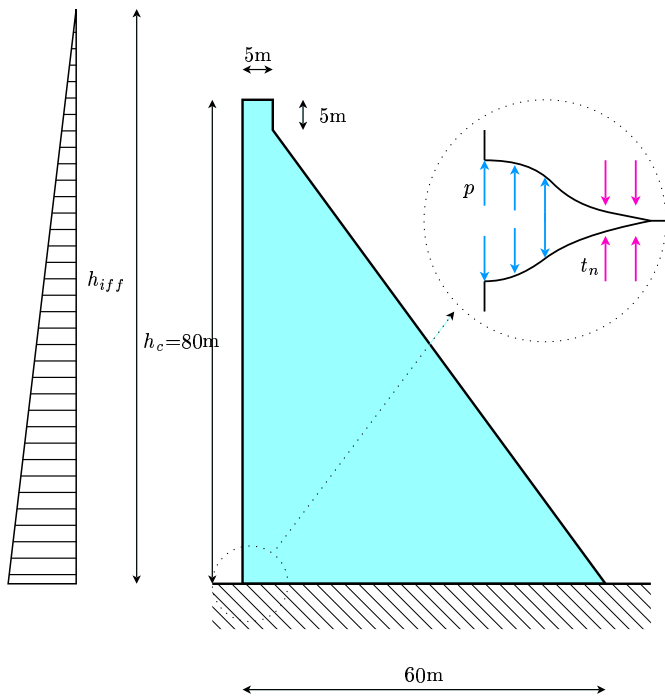
Figure 4. Gravity dam proposed as benchmark by ICOLD (1999).

Figure 5. Water lag vs. FCT position.

5.1 Water lag

The well established literature on water driven fracture (see Desroches, Detournay, Lenoach, Papanastasiou, Pearson, Thiercelin, and Cheng 1994) assume that the water penetrates into the crack but does not reach the FCT. The fraction of FPZ not reached by the water is called *water lag*. According to the experimental results of Reich, Brühwiler, Slowik, and Saouma 1994, it is assumed that the water penetrates into the FPZ up to the conventional knee point of the softening law ($w > w_{eff,c} \times 2/9 = 2.56 \times 2/9 = 0.569$ mm.) At the points where the water penetrates, the pressure is the same as in the reservoir at the same depth. The concrete and the rock are assumed to be impervious. The asymptotic expansion used is based on the assumption $\tau_{xy}|_{\theta=\pi} = -\mu_f \sigma_y|_{\theta=\pi}$ therefore it can be applied only in the region not reached by the water. Figure 5 shows the evolution of the water lag as a function of the FCT position.

5.2 Loading conditions

The dam is analysed under self-weight, reservoir filling and imminent failure flood loading conditions. In the numerical analysis the role of external load multiplier was played by the water level above the dam crest also called overtopping water heigth (shortening $h_{ovt} = h_{iff} - h_c$, see Fig. 4). Under the conservative assumptions previously described related to the material properties, the crack starts before the water level reaches the dam crest ($h_{ovt} < 0$).

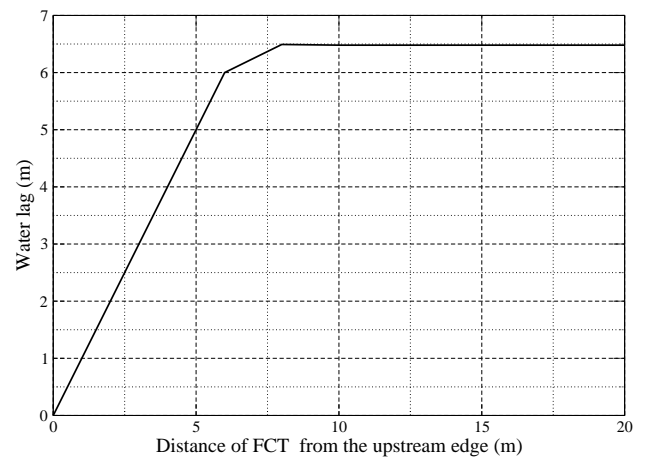Figure 6 shows the evolution of ($\tau/cohesion$) at the FCT as a function of the FCT position. Based on the

foregoing discussion, we can conclude that the associated load level h_{ovt} shown in Fig. 7 is just an overestimation of the real level. This model behaviour is due to the low value of cohesion suggested by the benchmark. For higher values of cohesion the solution shown in Fig. 8 and 7 is completely acceptable. Figure 7 gives the maximum value of h_{ovt} which is also the maximum load carrying capacity of the dam. Figure 8 shows the evolution of the horizontal crest displacement as a function of the FCT position and Fig. 9 the deformed mesh along the joint.
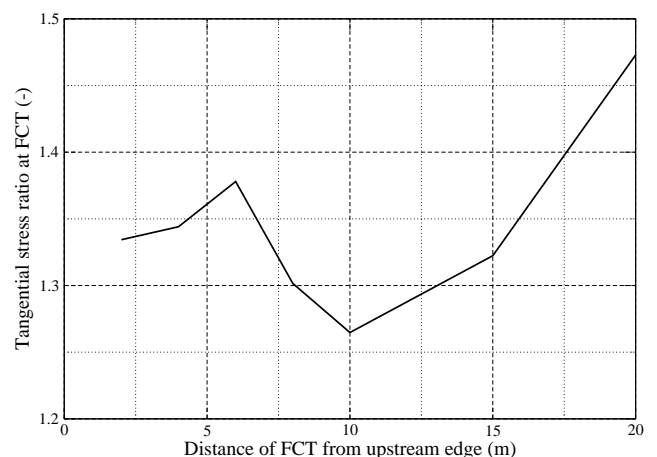

Figure 6. Tangential stress ratio τ_{xy}/cohesion at FCT vs. FCT position.
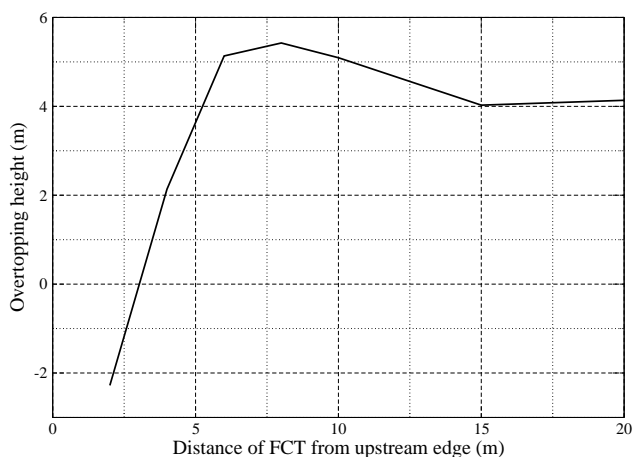
Figure 7. Overtopping height h_{ovt} vs. FCT position.
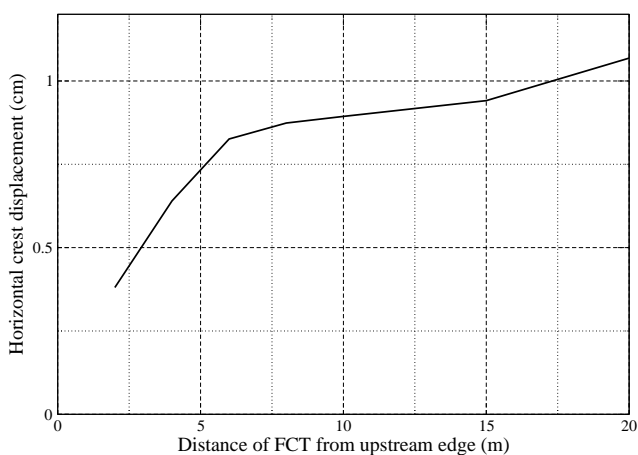

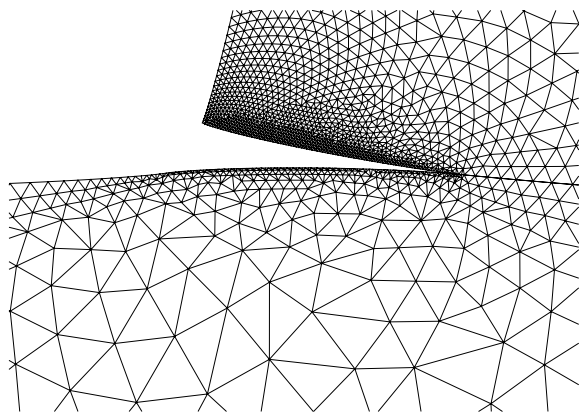Figure 8. Horizontal crest displacement vs. FCT position.

Figure 9. Deformed mesh.

6 CONCLUSIONS

- The reference volume involved in the fracture process of a dam joint is so large that it cannot be tested in a laboratory: a numerical model is needed.

- The use of the asymptotic expansions proposed by Karihaloo and Xiao 2008 at the tip of a crack with normal cohesion and Coulomb friction can overcome the numerical difficulties that appear in large scale problems when the Newton-Raphson procedure is applied to a set of equilibrium equations based on ordinary shape functions (Standard Finite Element Method).

- In this way it is possible to analyse problems with friction and crack propagation under the constant load induced by hydromechanical coupling.

- In the analysis of the dam-foundation joint penetrated by the water, for each position of the FCT, the condition K1=K2=0 allows us to obtain the external load level and the tangential stress at the FCT. If the joint strength is larger than the value obtained, the solution is acceptable, because the tensile strength is assumed negligible and the condition $K_1 = 0$ is sufficient to cause the crack growth. Otherwise the load level obtained can be considered as an overestimation of the critical value and a special form of contact problem have to be solved along the FPZ.

- For the boundary condition analysed, after an initial increasing phase, the water lag remains almost constant.

- For the boundary condition analysed, the maximun value of load carrying capacity is achieved when the water lag reaches its constant value.

7 ACKNOWLEDGMENTS

REFERENCES

Barpi, F. and S. Valente (2008). Modeling water penetration at dam-foundation joint. *Engineering Fracture Mechanics 75/3-4*, 629–642. Elsevier Science Ltd. (Great Britain).

Carol, I., P. Prat, and C. Lopez (1997). A normal/shear cracking model: Application to discrete crack analysis. *Journal of Engineering Mechanics (ASCE) 123(8)*, 765–773.

Cornelissen, H., D. Hordijk, and H. Reinhardt (1986). Experimental determination of crack softening characteristics of normal and lightweight concrete. *Heron 31*, 45–56.

Desroches, J., E. Detournay, B. Lenoach, P. Papanastasiou, J. Pearson, M. Thiercelin, and A. Cheng (1994). The crack tip region in hydraulic fracture. *Proceedings of the Royal Society of London A 447*, 39–48.

Gens, A., I. Carol, and E. Alonso (1990). A constitutive model for rock joints, formulation and numerical implementation. *Computers and Geotechnics 9*, 3–20.

ICOLD (1999). Theme A2: Imminent failure flood for a concrete gravity dam. In *Fifth International Benchmark Workshop on Numerical Analysis of Dams*, Denver (CO).

Karihaloo, B. and Q. Xiao (2007). Accurate simulation of frictionless and frictional cohesive crack growth in quasi-brittle materials using xfem. In A. Carpinteri, P. Gambarova, G. Ferro, and G. Plizzari (Eds.), *Sixth International Conference on Fracture Mechanics of Concrete and Concrete Structures (FRAMCOS6)*, pp. 99–110. Taylor and Francis (London).

Karihaloo, B. and Q. Xiao (2008). Asymptotic fields at the tip of a cohesive crack. *International Journal of Fracture 150*, 55–74.

Reich, W., E. Brühwiler, V. Slowik, and V. Saouma (1994). Experimental and computational aspects of a water/fracture interaction. The Netherlands, pp. 123–131. Balkema.

Sih, G. and H. Liebowitz (1968). Mathematical theories of brittle fracture. In H. Liebowitz (Ed.), *Fracture (vol. II)*, pp. 67–190. Academic Press (New York).

Strouboulis, T., K. Copps, and I. Babuska (2001). The generalized finite element method. *Computer Methods in Applied Mechanics and Engineering 190*, 4081–4193.

Červenka, J., J. Kishen, and V. Saouma (1998). Mixed mode fracture of cementious bimaterial interfaces; part ii: Numerical simulations. *Engineering Fracture Mechanics 60(1)*, 95–107.